

## Characterization of Synthesized Phenylthiazoly- liminomethyls and Some Metal-Complex Derivatives Irradiated with $\gamma$ -Rays

R.O. Aly<sup>#</sup>, R.S. Farag<sup>\*</sup> and M.M. Hassan<sup>\*</sup>

National Center for Radiation Research and Technology and

<sup>\*</sup>Chemistry Department, Faculty of Science, Al-Azhar University,  
Cairo, Egypt.

**T**WO SCHIFF-BASES I and II were prepared by the condensation reaction between the amine, 2-amino-4-phenylthiazole and the aldehydes salicylaldehyde and o-phthalaldehydic acid, respectively in 1:1 molar ratio. The metal-complex derivatives of Fe<sup>3+</sup>, Co<sup>2+</sup>, Ni<sup>2+</sup>, Cu<sup>2+</sup>, Zn<sup>2+</sup> and La<sup>3+</sup> were also prepared for each ligand. The elemental analysis, IR, UV-Visible, <sup>1</sup>H NMR and MS spectral analyses served the structure elucidation.

The products were  $\gamma$ -irradiated and the post-radiation UV-Visible results were studied. Some radiolysis products were suggested with the assistance, of the obtained MS results. The TGA events described the thermal stability and coordination establishment of the metal derivatives.

In association with the UV-Visible data and magnetic behavior of metal-complexes, the octahedral geometry was suggested for most of the investigated products. However, Cu-complexes revealed distorted arrangement. Most of the derivatives exhibited low molar conductance values illustrating the association of amines in the coordination sphere and the non-electrolyte behavior.

The antimicrobial activity tests showed significant inhibition against the Gram-positive *Bacillus subtilis* (NCTC-1040) by the Cu-complexes. Nevertheless, only the Cu-complexes of II displayed similarly against *Streptococcus pyogenes* (ATCC-19615). The Co-complex of II revealed also significant inhibition against the Gram-negative *E.coli* as well as against the fungus *Aspergillus fungatus*.

**Keywords:** Schiff-base, Metal-complex, Spectral analysis,  $\gamma$ -Irradiation and Antimicrobial activity.

Schiff-bases are characterized by the azomethine (-CH=N-) group. Thiazole and its derivatives play significant part in the animal kingdom. Vitamin B1, penicillin and coenzyme cocarboxylase contain the thiazole ring. Polyfunctional ligands based on benzazoles are relevant due to their biological activity as fungicides, antibiotics, pesticides and neuroprotectors<sup>(1,2)</sup>. Thiazole derivatives are widely used in the synthesis of the medicinal products such as sulphathiazole, an

---

<sup>#</sup>Corresponding author E-mail: raoufokasha@yahoo.co.uk

antibiotic<sup>(3)</sup>. Meanwhile, benzothiazoles are used for production of dyes with photosensitizing properties. Interaction of metal ions with N, O and S containing organic moieties has attracted much attention in the recent years. Such ligands and their complexes have been important due to the biological activity and the better understanding of metal protein binding. Hence, metal-complexes of Schiff-bases with heterocyclic compounds find applications as potential drugs<sup>(4,5)</sup>.

Most of the metal chelates have higher antimicrobial activity than the free ligands due to the lipophilic nature of the metal ions in complexes<sup>(6)</sup>. A number of works has been carried out with *o*-vanillin and 2-aminobenzothiazole metal-complexes<sup>(7-12)</sup>. The ligand system coordinates with the metal ion in a bidentate manner. Magnetic susceptibility data coupled with electronic spectra suggest that two ligands coordinate to the metal atom by phenolic oxygen and imino nitrogen to form high spin octahedral complex. The fifth and sixth positions of metal ion are satisfied with water molecules<sup>(13-17)</sup>.

A series of benzo[d] isothiazole, was synthesized and tested<sup>(18)</sup>. The compounds showed a marked cytotoxicity, compound concentration, 50 of 4–9  $\mu\text{M}$ , against the human CD4+ lymphocytes (MT-4) that were used to support HIV-1 growth. Thus, the most cytotoxic compounds of this series were evaluated for their antiproliferative activity against a panel of human cell lines derived from haematological and solid tumors. The results highlighted that all the derivatives inhibited the growth of leukaemia cell lines.

In this work two Schiff-bases were prepared by the condensation reaction between the aromatic amine 2-amino-4-phenylthiazole and aldehyde, namely salicylaldehyde and *o*-phthalaldehydic acid. Some ligand metal-complexes were synthesized and characterized by physicochemical and spectral analyses. Some title compounds were subjected to  $\gamma$ -radiation and the aftermath was spectrally investigated.

## Experimental

### Materials

All the employed chemicals were Merck-Germany, products. The Schiff-base implemented amine is 2-amino-4-phenylthiazole and the applied aldehydes are salicylaldehyde & *o*-phthalaldehydic acid. Metal-complexes were prepared by using the metal salts:  $\text{Fe}(\text{NO}_3)_3 \cdot 9\text{H}_2\text{O}$ ,  $\text{Co}(\text{CH}_3\text{COO})_2 \cdot 4\text{H}_2\text{O}$ ,  $\text{Ni}(\text{CH}_3\text{COO})_2 \cdot 4\text{H}_2\text{O}$ ,  $\text{Cu}(\text{CH}_3\text{COO})_2 \cdot \text{H}_2\text{O}$ ,  $\text{Zn}(\text{CH}_3\text{COO})_2 \cdot 2\text{H}_2\text{O}$  and  $\text{LaCl}_3 \cdot 7\text{H}_2\text{O}$ . Solvents and other used chemicals were of highly pure grade.

### Instruments

The IR spectra were recorded by Perkin Elmer 57928 RXIFT-IR system. Electronic absorption measurements were performed by Perkin Elmer lambda 35 UV- Visible spectrophotometer. The  $^1\text{H}$  NMR spectra were carried out by Varian, Gemini 200 MHz spectrometer. Hewlett Packard MS 5988 spectrometer was used for mass spectrometry. Thermal analysis was applied by Shimadzu 50.

Gamma-cell 220A was used for irradiation processes. Conductance Engineered System, U.S.A, was employed for the conductometric titration and molar conductance measurements.

*Preparation of Schiff-bases (I and II)*

The Schiff-bases (I and II) were prepared by the condensation reaction in which the aldehyde, 0.1 mole, was dropwisely added to the amine, 0.1 mole, with continuous stirring. Thereafter, the reaction mixture was heated at 100 °C for about 10 min in presence of 5 ml ethanol or acetic acid. The isolated yields were purified by recrystallization from a solvent (Table 1).

**TABLE 1. Analytical and physical data of Schiff-base (I-II)**

Compd No.	Product						
	Color	M.P. °C	M. F. M.Wt.	Elemental analysis Calcd. / Found			
				C %	H %	N %	S %
I	Dark yellow	158-160	C <sub>16</sub> H <sub>12</sub> N <sub>2</sub> OS 280	68.50	4.31	9.99	11.40
				67.80	4.56	9.23	11.50
II	Reddish white	163-165	C <sub>17</sub> H <sub>12</sub> N <sub>2</sub> O <sub>2</sub> S 308	66.20	3.92	9.08	10.40
				67.30	3.97	9.00	10.20

*Stoichiometry titration*

*Conductometric measurements:* The investigation was supported by the conductometric titration performed by titrating 10 ml of  $1 \times 10^{-3}$  M metal ion solution with increasing volume of  $1 \times 10^{-3}$  M complexing agent solution of Schiff-base derivatives using dimethyl sulfoxide (DMSO) as solvent and the conductance is then recorded after stirring the solution for about 2 min.

By plotting the conductance value, after correction for dilution as a result of addition of chelating agent, VS milliliters of the reagent added applying the least square equation for Y values according to the following equation<sup>(19)</sup>

$$Y = m X + b$$

where Y is conductance value, X is the volume of solution, m is the slope of curve and b is the intercept on the ordinate (y axis) Y usually the measured variable plotted as a function of changing as shown in Fig 1. The titration curves are smooth straight lines for all the points, and the well defined breaks are coincident with the stoichiometric ratio of complexes formed in solution.

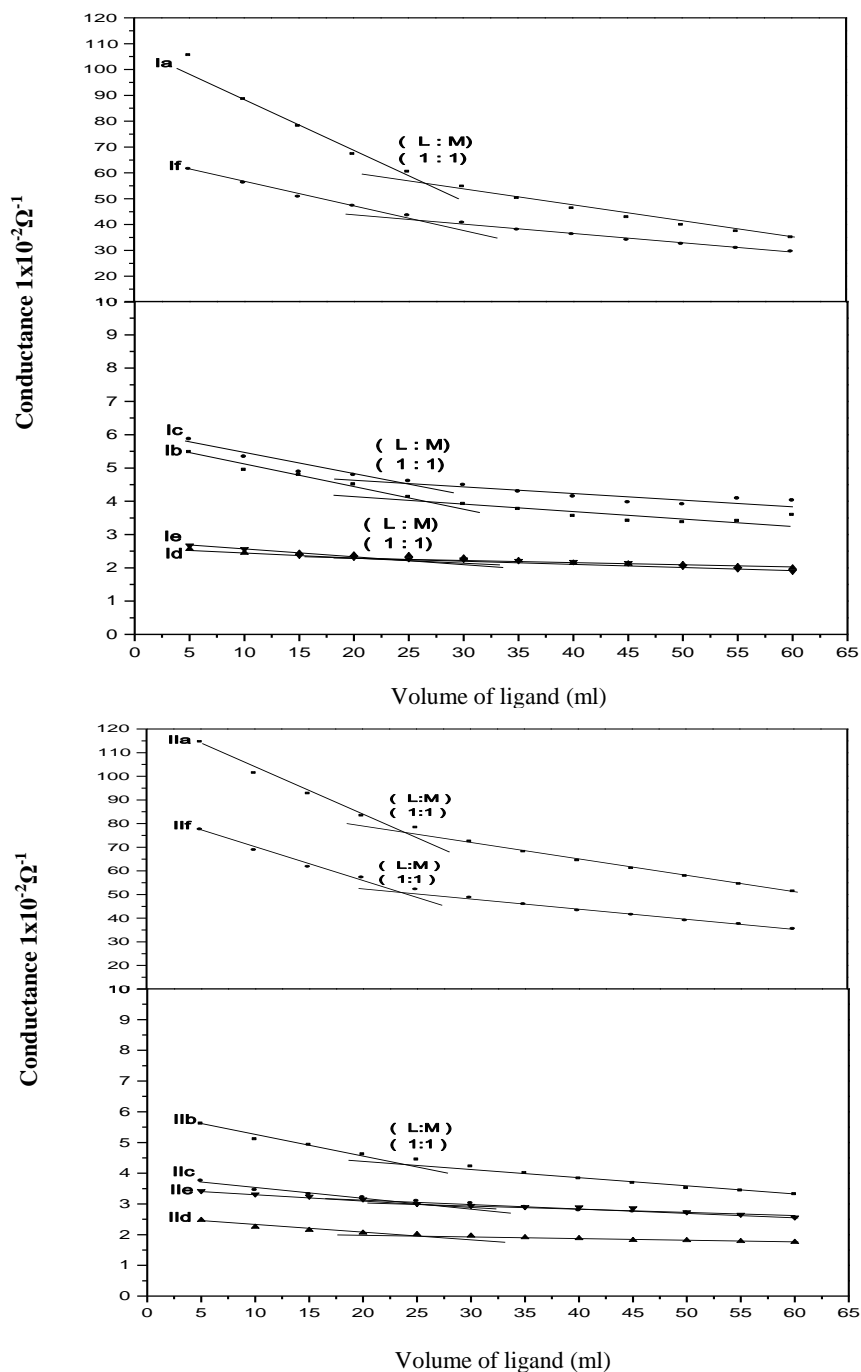


Fig.1. Conductometric titration curves for (I<sub>a-f</sub>-II<sub>a-f</sub>).

*Molar ratio method:* The molar ratio investigation was carried out by preparing 1.5 ml metal salt solutions kept constant at  $1 \times 10^{-3} \text{ M}$  in dimethyl formamide (DMF) while adding the ligand at a regular variable concentration of  $0.4\text{--}4 \times 10^{-3} \text{ M}$ .

The UV absorbance of the mixed solution was recorded at 302, 300, 306, 276, 307 and 316 nm for  $\text{Fe}^{3+}$ ,  $\text{Co}^{2+}$ ,  $\text{Ni}^{2+}$ ,  $\text{Cu}^{2+}$ ,  $\text{Zn}^{2+}$  and  $\text{La}^{3+}$ , respectively. The data are in good agreement with the (1:1) molar ratio suggested for these adducts

#### *Preparation of metal-complexes*

Metal-complexes were prepared by the addition of equimolar metal salt solution, 0.004 mole, to the Schiff-bases in 25 ml ethanol. Thereafter, the reaction mixture was heated under reflux for 6 hr. The solvent was then allowed to evaporate at room temperature (Table 2).

A complementary study based on the electronic absorption spectra and the magnetic moment measurement of metal-complexes, via Faraday method<sup>(20)</sup>, was employed to envisage the coordination geometry. The UV-Visible absorption within,  $\lambda_{\text{max}} = 200\text{--}1100 \text{ nm}$ , was examined for DMF  $10^{-5} \text{ M}$  solutions in the UV- and  $10^{-3} \text{ M}$  in the Visible- sector at room temperature. Meanwhile, the molar conductance of metal-complexes was detected in  $10^{-3} \text{ M}$  DMF solutions at room temperature.

#### *Irradiation process of ligands and complexes:*

Irradiation process were carried out for  $10^{-5} \text{ M}$  DMF solution in the UV-sector and  $10^{-3} \text{ M}$  in the Visible- sector, of selected synthesized substances by an integral gamma dose of 30 kGy at a dose rate of  $1.2 \text{ Gy s}^{-1}$  under ambient conditions. The post-radiation aftermath was followed up by UV-Visible spectral analysis at the above mentioned concentrations. The synthesized compounds were also tested for the antimicrobial activity using ampicillin as a reference<sup>(21)</sup>.

## **Results and Discussion**

#### *Schiff-base structure analysis*

The conformation of the synthesized Schiff-bases I and II was illustrated on the basis of the elemental analysis (Table 2) and the spectral data of IR, UV, NMR, MS.

#### *IR spectra*

The broad band at  $3334 \text{ cm}^{-1}$  was assignable for the O-H bond in I, and the weak at the region at  $2358 \text{ cm}^{-1}$  in II was accounted for the bonded one of the carboxylic group. Following this respect, the bands at  $3093$  and  $3096 \text{ cm}^{-1}$  are characteristic for the stretching vibrations of C-H aromatic bonds. The azomethine C-H bond was presented by the bands at  $2930$  and  $2825 \text{ cm}^{-1}$  in I and the weak at  $3009$  and  $2923 \text{ cm}^{-1}$  in II. Meanwhile, the broad band at  $3296 \text{ cm}^{-1}$  in the latter was ascribed to the stretching mode of vibration of  $\text{NH}^+$  generated by the Zewiter ion formation. Bands frequencies are attributed in Table 3.

**TABLE 2. Analytical and physical data of Schiff-base complexes (I-II).**

Compd. No.	Product					
	Color	M.P. °C	Yield/g (%)	M. F.	Elemental analysis	
					Calcd. /	Found
N %	M %					
I <sub>a</sub>	Dark brown	268-270	1.5 (75.75)	C <sub>16</sub> H <sub>15</sub> FeN <sub>4</sub> O <sub>9</sub> S	11.31 10.11	11.28 10.09
I <sub>b</sub>	Greenish yellow	218-220	1.4 (77.6)	C <sub>18</sub> H <sub>20</sub> CoN <sub>2</sub> O <sub>6</sub> S	6.21 5.62	13.06 11.98
I <sub>c</sub>	Reddish brown	189-193	1.35 (62.38)	C <sub>18</sub> H <sub>20</sub> N <sub>2</sub> NiO <sub>6</sub> S	6.21 5.96	13.01 13.73
I <sub>d</sub>	Brown	240-243	1.6 (91.53)	C <sub>18</sub> H <sub>18</sub> CuN <sub>2</sub> O <sub>5</sub> S	6.40 6.13	14.51 13.80
I <sub>e</sub>	Pale white	218-220	1.6 (87.52)	C <sub>18</sub> H <sub>20</sub> N <sub>2</sub> O <sub>6</sub> SZn	6.12 5.95	14.29 13.67
I <sub>f</sub>	Pale white	> 360	1.75 (83.33)	C <sub>16</sub> H <sub>15</sub> Cl <sub>2</sub> LaN <sub>2</sub> O <sub>3</sub> S	5.33 5.15	26.45 24.80
II <sub>a</sub>	Dark violet	280-282	1.45 (69.34)	C <sub>17</sub> H <sub>15</sub> FeN <sub>4</sub> O <sub>10</sub> S	10.71 10.34	10.76 11.10
II <sub>b</sub>	Pale violet	248-250	1.6 (83.5)	C <sub>19</sub> H <sub>20</sub> CoN <sub>2</sub> O <sub>7</sub> S	5.84 5.33	12.29 11.69
II <sub>c</sub>	Pale green	190-192	1.85 (96.55)	C <sub>19</sub> H <sub>20</sub> N <sub>2</sub> NiO <sub>7</sub> S	5.85 5.17	12.25 12.27
II <sub>d</sub>	Brown	295-297	1.5 (80.64)	C <sub>19</sub> H <sub>18</sub> CuN <sub>2</sub> O <sub>6</sub> S	6.01 5.28	13.64 12.87
II <sub>e</sub>	White	173-175	1.15 (59.28)	C <sub>19</sub> H <sub>20</sub> N <sub>2</sub> O <sub>7</sub> SZn	5.77 5.13	13.46 13.25
II <sub>f</sub>	Greenish white	212-215	1.65 (74.59)	C <sub>17</sub> H <sub>15</sub> Cl <sub>2</sub> LaN <sub>2</sub> O <sub>4</sub> S	5.06 4.70	25.11 24.30

**TABLE 3. Characteristic IR stretching vibration (cm<sup>-1</sup>) of Schiff-base (I-II)**

Compd No.	Stretching vibration in cm <sup>-1</sup>							
	νO-H	νC-H <sub>Ar</sub>	νC-H <sub>Al</sub>	νC=O	νC=N	νC=C	νC-N	νC-S-C
I	3334	3093	2930 2825	-----	1602	1514	1334	752
II	3296	3096	3009 2923	1750	1556	1470	1336	764

The bands at 1602 and 1556  $\text{cm}^{-1}$  were ascribed to the stretching mode of the azomethine bond, C=N, whereas, the bands at 1514 and 1470  $\text{cm}^{-1}$  were accounted for the C=C bond in I and II, respectively. The band at 1456  $\text{cm}^{-1}$  in the former was referred to the C-H deformation, whilst that at 1750  $\text{cm}^{-1}$  in the latter was confirmatory for the carboxylic group C=O bond. Meanwhile, the band located at 1230  $\text{cm}^{-1}$  in I was significant for the C-O bond. The C-N bond was demonstrated by the bands at 1334 and 1336  $\text{cm}^{-1}$  in I and II, respectively, whereas the bands at 752 and 764  $\text{cm}^{-1}$  were referred to the C-S-C bonds in the same respect.

#### Electronic absorption spectra (UV-visible)

The electronic absorptions of the Schiff-bases I and II, respectively, revealed the following results:  $\lambda_{\text{max}} = 204\text{-}246, 204\text{-}244$  nm each region exhibits the phenyl ring transition ( ${}^1L_a \leftarrow {}^1A$ ), whereas the bands at 259 and 255 nm demonstrate the phenyl ring transition ( ${}^1L_b \leftarrow {}^1A$ ). The  $\pi\text{-}\pi^*$  transitions of the C=N group were displayed by  $\lambda_{\text{max}} = 270$  nm in both compounds. Similarly, in I, the C=O group showed the absorption peak at  $\lambda_{\text{max}} = 232$  nm. The broad peak at  $\lambda_{\text{max}} = 331$  and 330 nm, respectively, was referred to the n- $\pi^*$  transition of the azomethine group and the carbonyl group in II.

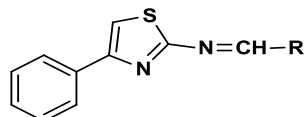
#### ${}^1\text{H}$ NMR spectra

The Schiff-bases I and II, dissolved in DMSO- $d_6$ , were examined by  ${}^1\text{H}$  NMR. The hydroxyl proton of the phenol in I and the aromatic acid in II was reported by a singlet at  $\delta$  11.6 and  $\delta$  9 which disappeared by the addition of  $\text{D}_2\text{O}$ . Within the range  $\delta$  6.8-7.8 the aromatic protons of the two different phenyl rings in both compounds displayed multiplet signals. The azomethine proton was reported by a singlet at  $\delta$  7.86 and  $\delta$  7.88, respectively.

#### Mass spectra (MS)

The mass spectra of the two Schiff-bases I and II exhibited the following data. The molecular peak was respectively reported for I and II at  $m/e = 280$  (58.8%) and 308 (13.9%). The compound I revealed also the ion peak at  $m/e = 263$  (28.4%) for  $\text{M}^+(\text{C}_{16}\text{H}_{11}\text{N}_2\text{S})$ ,  $m/e = 247$  (57.7%) for  $\text{M}^+(\text{C}_{16}\text{H}_{11}\text{N}_2\text{O})$ ,  $m/e = 203$  (16.5%) for  $\text{M}^+(\text{C}_{10}\text{H}_7\text{N}_2\text{OS})$ ,  $m/e = 176$  (100%) for the base  $\text{M}^+(\text{C}_9\text{H}_8\text{N}_2\text{S})$ ,  $m/e = 134$  (73.9%) for  $\text{M}^+(\text{C}_8\text{H}_6\text{S})$ ,  $m/e = 102$  (62%) for  $\text{M}^+(\text{C}_8\text{H}_6)$ ,  $m/e = 89$  (29.9%) for  $\text{M}^+(\text{C}_7\text{H}_5)$  and  $m/e = 77$  (33.3%) for  $\text{M}^+(\text{C}_6\text{H}_5)$ . Meanwhile, compound II showed the base peak by  $m/e = 133$  (100%) for  $\text{M}^+(\text{C}_8\text{H}_5\text{S})$ . Furthermore, the ion peak at  $m/e = 102$  (7.4%) was assigned for  $\text{M}^+(\text{C}_8\text{H}_5)$ , and  $m/e = 77$  (45.8%) for  $\text{M}^+(\text{C}_6\text{H}_5)$ .

The collected data from the elemental and spectral analyses may illustrate the following structures:



where R is o-C<sub>6</sub>H<sub>5</sub>-OH in I: 2-((5-phenylthiazol-2-ylimino) methyl) phenol and o-C<sub>6</sub>H<sub>5</sub>-COOH in II: 2-((5-phenylthiazole-2-ylimino) methyl) benzoic acid.

#### *Elucidation of metal –complex structure*

Schiff-base metal-complexes I<sub>a-f</sub> and II<sub>a-f</sub> were produced using the metal ions Fe<sup>3+</sup>, Co<sup>2+</sup>, Ni<sup>2+</sup>, Cu<sup>2+</sup>, Zn<sup>2+</sup> and La<sup>3+</sup>, respectively. Suggestion of the metal-complex conformation was provided by the elemental (Table 2), and spectral analyses.

#### *IR spectra*

In comparison with the parent ligand the common bands shift to lower or higher frequency with concomitant change in intensity. In addition, metal-nitrogen bonds were found common in the coordination compound.

With respect to the order of metal ions the weak broad bands at 3332, 3472, 3398, 3354, 3381 and 3418 cm<sup>-1</sup> in I<sub>a-f</sub> and at 3408, 3446, 3478, 3476, 3300 and 3360 cm<sup>-1</sup> in II<sub>a-f</sub> were assigned for the associated water molecules. The weak bands observed at 3109, 3038, 3094, 3065 and 3158 cm<sup>-1</sup> in I<sub>a-e</sub> and at 3106, 3075, 3138, 3074, 3104 and 3122 cm<sup>-1</sup> in II<sub>a-f</sub> were attributed to the aromatic C-H bond. Further, the appearance of the bands located at 1386, 1440, 1438, 1436, 1440 and 1459 cm<sup>-1</sup> in I<sub>a-f</sub> and at 1386, 1428, 1420, 1442 and 1444 cm<sup>-1</sup> were ascribed also to the in-plane bending deformation of the aromatic C-H bond.

Meanwhile, the C-H aliphatic bond of the azomethine and the acetate group, in the acetate containing complexes, demonstrated weaker and lower shifted bands located at 2996, 2942, 2934, 2930 and 3062 cm<sup>-1</sup> in I<sub>a-e</sub> and at 2948, 2991, 2943, 2938, 2940 and 2735 cm<sup>-1</sup> in II<sub>a-f</sub>. As incorporated in the coordination sphere the azomethine bond exhibited shifts to lower frequencies. In I<sub>a-f</sub> the band was shifted to 1528, 1562, 1568, 1526, 1522 and 1628 cm<sup>-1</sup> and in II<sub>a-f</sub> to 1658, 1580, 1526, 1604, 1528 and 1638 cm<sup>-1</sup>. The acetate complexes exhibited for  $\nu_{as} \text{COO}^-$  the bands at 1575, 1574, 1600 and 1600 cm<sup>-1</sup> in I<sub>b-e</sub> and at 1700, 1702, 1690 and 1628 cm<sup>-1</sup> in II<sub>b-e</sub>. In addition, the  $\nu_{sym} \text{COO}^-$  was displayed by the bands observed at 1344, 1338, 1378 and 1380 cm<sup>-1</sup> in I<sub>b-e</sub> and at 1350, 1346, 1300 and 1340 cm<sup>-1</sup> in II<sub>b-e</sub>.

The C-S-C bonds revealed the bands appeared at 694, 676, 684, 696 and 714 cm<sup>-1</sup> in I<sub>a-f</sub> and at 690, 680, 682, 694, 700 and 702 cm<sup>-1</sup> in II<sub>a-f</sub>. The coordination bond M←N displayed the bands at 606, 616, 618, 619, 590 and 544 cm<sup>-1</sup> in I<sub>a-f</sub> and at 626, 616, 628, 630, 528 and 606 cm<sup>-1</sup> in II<sub>a-f</sub>. Furthermore, the M←O coordination bond demonstrated the bands at 466, 488, 528, 529 and 528 cm<sup>-1</sup> in I<sub>a-e</sub> and at 474, 490, 554, 466 and 542 cm<sup>-1</sup> in II<sub>a-d, f</sub>.

The II<sub>a-f</sub> spectra confirmed the carbonyl bond in the carboxylic group by the reported bands located at 1772, 1764, 1756, 1760, 1789 and 1752 cm<sup>-1</sup>.

*UV-visible and magnetic behavior: coordination geometry*

As a result of the isolating effect of the ligand the magnetic properties of metal-complexes yield direct information on the electronic configuration of the central ions, oxidation state of metal ion and the number of unpaired electrons of the d-shell.

The measured magnetic moment of Fe (III)-complexes I<sub>a</sub>, II<sub>a</sub>,  $\mu_{\text{eff}} = 5.03\text{-}6.02$  B.M., suggested the octahedral, low-spin, geometry. The coordination geometry was supported by three bands within  $\lambda_{\text{max}} = 367\text{-}606$  nm that are assignable for  ${}^6A_1 \rightarrow {}^4T_1$  (G),  ${}^6A_1 \rightarrow {}^4E_g$ ,  ${}^4A_1$  (G) and  ${}^6A_1 \rightarrow {}^4E_g$  (D) transitions.

The high-spin octahedral Co (II)-complexes I<sub>b</sub> and II<sub>b</sub> possess three unpaired electrons, however, they may be distinguished by the magnitude of deviation of  $\mu_{\text{eff}}$  from the spin-only value<sup>(22)</sup>. The measured magnetic moment,  $\mu_{\text{eff}} = 4.0\text{-}4.41$  B.M., shades light on the presence of three unpaired electrons indicating a high-spin octahedral configuration. This is supported by the band within the region  $\lambda_{\text{max}} = 356\text{-}441$  nm representing the  ${}^4T_1 \rightarrow {}^4T_1$  (P) transitions in I<sub>b</sub> and II<sub>b</sub> complexes.

The measured magnetic moment for Ni (II)-complexes I<sub>c</sub> and II<sub>c</sub>,  $\mu_{\text{eff}} = 2.84\text{-}3.18$  B.M., is of high-spin at room temperature and consistent within the observed normal range for octahedral Ni (II)-complexes.<sup>(23)</sup> The suggested configuration is supported by the appearance of three bands within the region  $\lambda_{\text{max}} = 375\text{-}498$  nm in I<sub>c</sub> and II<sub>c</sub>. As the ground state of Ni (II) in an octahedral coordination is  ${}^3A_2$ , the exhibited bands may be assigned to the  ${}^3A_2$  (F)  $\rightarrow$   ${}^3A_2$  (P) transition.

The measured magnetic moment for Cu (II)-complexes I<sub>d</sub> and II<sub>d</sub>,  $\mu_{\text{eff}} = 1.7\text{-}1.85$  B. M., at room temperature is consistent within the range normally observed for distorted octahedral<sup>(24)</sup>. The  ${}^2E_g$  and  ${}^2T_{2g}$  states of the octahedral  $\text{Cu}^{+2}$  ion ( $d^9$ ,  ${}^2D$  term) split under the influence of the tetragonal distortion due to ligand field and Jan-teller distortion effect.<sup>(25)</sup> By distortion three spin allowed transitions are expected:  ${}^2B_{1g} \rightarrow {}^2A_{1g}$ ,  ${}^2B_{1g} \rightarrow {}^2B_{2g}$  and  ${}^2B_{1g} \rightarrow {}^2E_g$ . The Cu-complexes I<sub>d</sub> and II<sub>d</sub> displayed bands in the region  $\lambda_{\text{max}} = 375\text{-}500$  nm referred to  ${}^2B_{1g} \rightarrow {}^2B_{2g}$  and  ${}^2B_{2g} \rightarrow {}^2E_g$  transitions. The Zn- and La-complexes are diamagnetic possessing the octahedral coordination. Measured magnetic moments are tabulated in Table 4

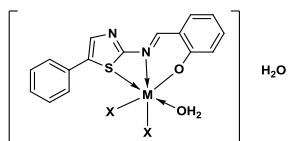
*<sup>1</sup>H NMR spectra*

<sup>1</sup>H NMR spectra of Zn-complexes I<sub>e</sub> and II<sub>e</sub> were recorded in DMSO-d<sub>6</sub>. The absorption of the azomethine proton was demonstrated by a singlet of less intensity than shown for the parent ligands shifted at  $\delta$  7.6 in I<sub>e</sub> and  $\delta$  7.96 in II<sub>e</sub>. The discrepancy in appearance was accounted for the establishment of coordination. Aromatic protons displayed multiplets within  $\delta$  6.8-7.5 in I<sub>e</sub> and  $\delta$  6.8-7.8 in II<sub>e</sub>. The methyl proton in the acetate group revealed a shift at  $\delta$  1.83 in I<sub>e</sub> and at  $\delta$  1.84 in II<sub>e</sub>. Furthermore, the disappearance of the hydroxyl proton in I<sub>e</sub> and the carboxylic proton in II<sub>e</sub> shades light on the involvement of the hydroxyl groups in the complexation process of both.

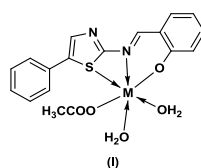
TABLE 4. The magnetic properties of the metal Schiff-base complexes

Complex		$\mu_{\text{eff}}$ (B. M.)
No.	Metal	
I <sub>a</sub>	Fe	6.02
I <sub>b</sub>	Co	4.29
I <sub>c</sub>	Ni	2.90
I <sub>d</sub>	Cu	1.74
I <sub>e</sub>	Zn	Diamagnetic
I <sub>f</sub>	La	Diamagnetic
II <sub>a</sub>	Fe	5.74
II <sub>b</sub>	Co	4.0
II <sub>c</sub>	Ni	2.86
II <sub>d</sub>	Cu	1.7
II <sub>e</sub>	Zn	Diamagnetic
II <sub>f</sub>	La	Diamagnetic

In view of the above mentioned analyses, the following conformations may be suggested for the metal-complexes I<sub>a-f</sub> and II<sub>a-f</sub>.

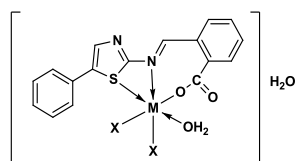


I<sub>a</sub>; M= Fe<sup>3+</sup>, X=NO<sub>3</sub>  
I<sub>f</sub>; M= La<sup>3+</sup>, X=Cl

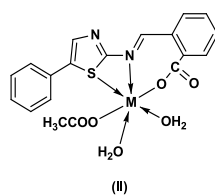


I<sub>b</sub>; M= Co<sup>2+</sup>, X=Aco  
I<sub>c</sub>; M= Ni<sup>2+</sup>, X= Aco  
I<sub>d</sub>, M = Cu<sup>+2</sup>, X =Aco  
I<sub>e</sub>; M= Zn<sup>2+</sup>, X=Aco

M



II<sub>a</sub>; M= Fe<sup>3+</sup>, X=NO<sub>3</sub>  
II<sub>f</sub>; M= La<sup>3+</sup>, X=Cl



II<sub>b</sub>; M= Co<sup>2+</sup>, X=Aco  
II<sub>c</sub>; M= Ni<sup>2+</sup>, X= Aco  
II<sub>d</sub>; M= Cu<sup>2+</sup>, X=Aco  
II<sub>e</sub>; M= Zn<sup>2+</sup>, X=Aco

### Miscellaneous behaviors

#### $\gamma$ -Irradiation stability

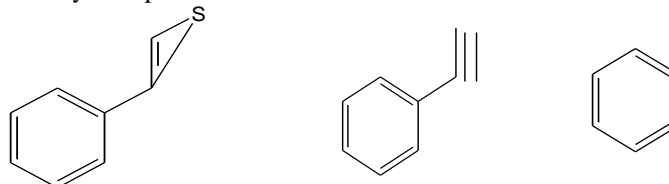
Ligand I and II in DMF solution were  $\gamma$ -irradiated at conditions of:  $10^{-5}\text{M}$ , neutral medium, ambient air and room temperature by 30 kGy total integral dose and  $1.2\text{ Gy s}^{-1}$  dose rate. At relatively low dose rate, the linear energy transfer favors the non-interradical reactions<sup>(26)</sup>, and the excitation energy received by the aromatic systems is channeled to relatively low-energy triplet excited states which have a low probability of dissociation<sup>(27)</sup>.

Little have been published concerning the radiolysis of aromatic alcohols and phenols. However, in analogy with aliphatic alcohols, the radiolysis reaction tends to center on the oxygen functional group rather than on the hydrocarbon chains(s), the bond scission is predominantly C-H and O-H<sup>(28)</sup>. Also, as with the alcohols and ethers, radiolysis of the carbonyl compounds and carboxylic acids and their derivatives centers on the functional groups and adjacent carbon atoms. Rupture of a C-O bond and loss of  $\alpha$ -hydrogen occur with the decarboxylation with the acids and elimination of CO and CO<sub>2</sub> with the esters<sup>(29)</sup>. Generally, aromatic radicals generally combine rather than disproportionate<sup>(30)</sup>.

Analogous to  $\gamma$ -radiolysis of acetone at a relatively low dose rate,  $0.81\text{ Gy s}^{-1}$ , DMF methyl radicals, likely to attack the substrate giving various yields, may also produce similar products, *e.g.* H<sub>2</sub>, H<sub>4</sub>, and CO<sup>(31)</sup>.

In general, the influence of  $\gamma$ -irradiation on the ligands I and II was represented by variation in the resolution of the pristine spectra. The phenylic transition region, within  $\lambda_{\text{max}} = 200\text{-}260\text{ nm}$ , exhibited better and diverse resolved characters, whereas within  $\lambda_{\text{max}} = 260\text{-}320\text{ nm}$ , less resolved, and larger absorbance in the case of II, species were detected in association with the disappearance of the C=N  $n\text{-}\pi^*$  transition at 330 nm in both ligands. The results may suggest the generation of various aromatic structures in addition to the formation of longer and distinctive conjugated systems as a result of the cleavage of the azomethine bond and the likelihood of aromatic radical-radical recombinations.

With the guidance of the MS products, as a first approach, three potential radiolysis products may be represented<sup>(32)</sup>:



Postulated radiation-induced species

The metal complexes I<sub>a-d</sub> and II<sub>a-d</sub> exhibited nearly similar behavior within the region  $\lambda_{\text{max}} = 200\text{-}360\text{ nm}$  where the phenylic and  $\pi\text{-}\pi^*$  transitions demonstrated a number of resolved figures. Meanwhile, within the visible region at a

concentration of  $10^{-3}$  M, in contrast with the UV-region data, the resolved bands within the region  $\lambda_{\text{max}} = 370\text{-}550$  nm turned out to fine resolved species. Evidently, distortion of the complex structure by irradiation is definite at the applied conditions leading to the formation of various distinctive structures demonstrated by multi resolved fine spectral shapes<sup>(33)</sup>.

#### *Thermal stability*

Co (II) metal-complex  $I_b$  demonstrated a four- staged thermogram. A weight loss of 3.52% at  $100^\circ\text{C}$  was accounted for a loss of one molecule of crystallization water. The next stage, within the temperature range  $130\text{-}220^\circ\text{C}$ , showed a loss of 13.44% revealing the isolation of an acetate group. The third stage of 34.18% loss within the range  $250\text{-}360^\circ\text{C}$  was attributed to the loss of  $[\text{C}_9\text{H}_5\text{NS}]$  adduct. Eventually, the fourth step a residue of 45% of the original weight was stable up to  $1000^\circ\text{C}$ .

The La (III) metal-complex  $II_f$  revealed a five-staged thermogram. The first weight loss of 1.52% was observed within the region  $50\text{-}90^\circ\text{C}$  and was attributed to the loss of a half molecule of crystallization water. The following loss was of 2.69% within the range  $90\text{-}190^\circ\text{C}$  corresponding to the loss of one crystallization water molecule. Within the range  $190\text{-}290^\circ\text{C}$ , a loss of 6.45% was detected and was accounted for the loss of one chlorine atom. The fourth stage of 27% loss within the range  $290\text{-}500^\circ\text{C}$  was referred to the loss of the adduct  $[\text{C}_8\text{H}_6\text{NO}_2]$ . The last stage suggested the loss of the adduct  $[\text{C}_{11}\text{H}_{18}\text{N}_2\text{O}_2\text{S}]$ , whilst the remanant residue was of 19.3% could withstand to  $1000^\circ\text{C}$ .

#### *Molar conductance*

The molar conductance of the complexes was determined in  $10^{-3}$ M DMF solution at room temperature. The metal-complexes of Fe, Co, Ni, Cu, Zn and La,  $I_{a-f}$ , respectively revealed 141, 27.4, 29.2, 24.1, 11 and  $173 \Omega^{-1} \text{cm}^2 \text{mol}^{-1}$ . Meanwhile,  $II_{a-f}$  showed the molar conductance yields of 252, 16.8, 22.5, 23.3, 27.2 and  $190.5 \Omega^{-1} \text{cm}^2 \text{mol}^{-1}$ . The predicated low values for  $I_{b-e}$  and  $II_{b-e}$  may suggest the involvement of the associated amines in the coordination sphere in each. Thus, the complexes are neutral and behave as non-electrolytes. The retained values for  $II_{a,f}$  indicate 1:2 electrolyte suggesting the ionic nature<sup>(34)</sup>.

#### *Antimicrobial activity*

The metal-complexes  $I_{a-f}$  and  $II_{a-f}$  were examined employing ampicillin as a reference while dissolved by 1g/ml DMSO. Against the Gram-positive *Bacillus subtilis* (NCTC-1040),  $I_d$  and  $II_d$  showed significant inhibition. Whilst,  $II_b$  showed a moderate inhibition and the weak inhibition was revealed by  $I_c$ . Further, against *Streptococcus pyogenes* (ATCC-19615),  $II_d$  demonstrated significant inhibition, while  $II_b$  revealed moderate inhibition Co and Cu samples  $I_{b,d}$  yielded weak inhibition.

The Gram-negative bacteria investigations showed the following: for *E.coli*, only  $II_b$  exhibited significant inhibition. For Clostridium,  $I_f$  and  $II_f$  showed moderate inhibition, whereas  $I_d$  and  $II_d$  revealed inhibition. The antifungal  
*Egypt. J. Chem.* **54**, No. 6 (2011)

behavior was investigated and Clofran served as a reference. Against *Aspergillus fungates*, II<sub>b</sub> and II<sub>d</sub> showed significant and moderate inhibition, respectively.

### Conclusions

The chemical structure of the two Schiff-bases I and II and metal-complex derivatives I<sub>a-f</sub> and II<sub>a-f</sub> was illustrated and verified via elemental and spectral analyses. The metal-complexes revealed new IR vibrations confirming the establishment of the coordination process. Additionally, the argument based on the association of the magnetic behavior with the reported UV-Visible data showed the domination of the octahedral arrangement with the exception of the Cu-complexes which revealed distorted geometry.

It can be concluded that the  $\gamma$ -irradiation process at the applied condition resulted in a destructive impact on the coordination system in the metal-chelates as inferred by the UV-Visible post-radiation traces. The radiolysis of the ligand and metal-complex substrates as well as the employed solvent was discussed and some presumably formed species were postulated.

TGA traces asserted the involvement of the crystallization water molecules in the coordination sphere. Most of the metal-complexes, namely I<sub>b-e</sub> and II<sub>b-e</sub> showed low molar conductance values corroborating the association of anions in the coordination sphere and those metal-complexes behave as non-electrolytes. Meanwhile II<sub>a,f</sub> exhibited 1:2 electrolyte suggesting the ionic nature. In addition, the antimicrobial activity tests revealed significant inhibition by I<sub>d</sub> and II<sub>d</sub> against the Gram-positive, *Bacillus subtilis* (NCTC-1040). Similarly, II<sub>d</sub> was effective against *Streptococcus pyogenes* (ATCC-19615). Against the Gram-negative, *E. coli*, only II<sub>b</sub> gave also similar impact as well as against the fungus *Aspergillus fungatus*.

### References

1. Ramalingan, C., Balasubramanian, S., Kabilan, S. and Vasudevan, M., Synthesis and study of antibacterial and antifungal activities of novel 1-[2-(benzoxazol-2-yl)ethoxy]-2,6-diarylpiperidin-4-ones. *Eur. J. Med. Chem.* **39**, 527 (2004)
2. Zitouni, G.T., Demirayak, S., Ozdemir, A., Kaplancikli, Z.A. and Yildiz, M.T., Synthesis of some 2-[(benzazole-2-yl)thioacetyl amino]thiazole derivatives and their antimicrobial activity and toxicity. *Eur. J. Med. Chem.* **39**, 267 (2003).
3. Borisenko, V.E., Koll, A., Kolmakov, E.E. and Rjasnyi, A.G., Hydrogen bonds of 2-aminothiazoles in intermolecular complexes (1:1 and 1:2) with proton acceptors in solutions. *J. Mol. Struct.* **783**, 101 (2004).
4. Konstantinivi, S.S., Radovanovi, B. C., Caki, Z. and Vasic, V., Synthesis and characterization of Co(II), Ni(II), Cu(II) and Zn(II) complexes with 3-salicylidenehydrazono-2-indolinone. *J. Ser. Chem. Soc.* **68**, 641 (2003).

5. **Anderson, O.**, Principles and recent developments in chelation treatment of metal intoxication. *Chem. Rev.* **99**, 2683 (1999).
6. **Raman, N., Raja, Y. P. and Kulandaisamy, A.**, Synthesis and characterisation of Cu(II), Ni(II), Mn(II), Zn(II) and VO(II) Schiff base complexes derived from o-phenylenediamine and acetoacetanilide. *Proc. Indian Acad. Sci. (Chem. Sci.)* **113**, 183 (2001).
7. **Tellez, F., Pena-Hueso, A., Barba-Behrens, N., Contreras, R. and Flores-Parra, A.**, Coordination compounds in a pentacyclic aromatic system from 2-aminobenzothiazole derivatives and transition metal ions. *Polyhedron*, **25**, 2363 (2006).
8. **Tellez, F., Flores-Parra, A., Barba-Behrens, N. and Contreras, R.**, Cobalt (II) and zinc (II) compounds with unsaturated ligands derived from 2-aminobenzothiazole. *Polyhedron*, **23**, 2481 (2004).
9. **Sokolowska-Gajda, J., and Freeman, H.S.**, A new medium for the diazotization of 2-amino-6-nitrobenzothiazole and 2-aminobenzothiazole. *Dyes Pigments*, **20**, 137 (1992).
10. **Giusti, G.**, Peyronel, spectrochim. zinc(II), cadmium(II) and mercury(II) complexes of 2-aminobenzothiazole. *Acta A* **38**, 975 (1982)
11. **Yin, H.D. and Chen, S.W.**, Synthesis and characterization of organotin(IV) compounds with Schiff base of o-vanillin-2-thiophenylhydrazone. *J. Organomet. Chem.* **691**, 3103 (2006).
12. **Velcheva, E.A. and Stamboliyska, B.A.**, IR spectral and structural changes caused by the conversion of 3-methoxy-4-hydroxybenzaldehyde (vanillin) into the oxyanion. *Spectrochim. Acta*, **A60**, 2013 (2004).
13. **Nair, M.S., Sudakumari, S. and Neelakantan, M.A.**, Studies on some novel Schiff-base complexes in solution and solid state. *J. Coord. Chem.* **60**, 1291 (2007).
14. **Nair, M.S. and Neelakantan, M.A.**, Inorganic chemistry-multiple equilibria involved in some nickel(II) mixed ligand complex systems containing catecholic and dipeptide ligands. *J. Indian Chem. Soc.* **77**, 23 (2000).
15. **Neelakantan, M.A., Marriappan, S.S., Dharmaraja, J., Jeyakumar, T. and Muthukumaranc, K.**, Spectral, XRD, SEM and biological activities of transition metal complexes of polydentate ligands containing thiazole moiety. *J. Spectrochimica Acta . Part A*, **71**, 628 (2008).
16. **Vicini, P., Geronikaki, A., Incerti, M., Busonera, B., Poni, G., Cabras, C.A. and Colla, P.L.**, Synthesis and biological evaluation of benzo[d]isothiazole, benzothiazole and thiazole Schiff bases. *J. Bioorg. Med. Chem.* **11**, 4785–4789 (2003)
17. **Aly, R.O., Farag, R.S. and Hassan, M.M.**,  $\gamma$ -Irradiation and characterization of synthesized methoxybenzylpyrimidine formimidate Schiff -base and some metal-complex derivatives. *Arabian Journal of Chemistry*. doi:10.1016/j. arabjc.09. 017 (2011).
18. **Bates, L.F.**, "Modern Magnetism" 2<sup>nd</sup> ed. Cambridge at the University Press (1948).

19. **Hewitt, W. and Vincent, S.**, *Theory and Application of Microbiological Array* publishes Academic press, INC. New York (1989).
20. **Cotton, F.A. and Wilkinson, G.**, *Advanced Inorganic Chemistry Book* (Wiley Interscience), New York, 5<sup>th</sup> ed. 725 (1988).
21. **Kumar, R.S., Nethiji, M. and Patil, K.C.**, Preparation, characterization, spectral and thermal analyses of  $(N_2H_5)_2MCl_4 \cdot 2H_2O$  (M = Fe, Co, Ni and Cu); crystal structure of the iron complex. *polyhedron*, **10**, 365 (1991)
22. **Miessler, G.L. and Tarr, D.A.**, In: *Inorganic Chemistry* (3<sup>rd</sup> d) book, Pearson Prentice Hall (2004).
23. **Baxendale, J.H. and Wardman, P.**, The radiolysis of methanol [electronic resource]: product yields, rate constants, and spectroscopic parameters of intermediates. U.S. Dept. Commerce-National Bureau of Standards, Washington, DC. (1975)
24. **Burns, W.G. and Barker, R.** *Aspects of Hydrocarbon Radiolysis Book* (T. Gaumann and J. Hoigne Ed.), Academic, NY, Ch. 2. (1968)
25. **Tepley, J.**, Chemistry of alcohols, ethers and ketones in condensed states. *Radiat. Res. Rev.* **1**, 361 (1969)
26. **Sumiyoshi, T., Tsugaru, K., Yamada, T. and Katayama, M.**, Yields of solvated electrons at 30 Picoseconds in water and alcohols. *Bull. Chem. Soc. Jpn.* **58**, 3073 (1985)
27. **Proskurnin, M.A. and Barelko, E.V.**, *Proc. Int. Conf. Peaceful Uses Atomic Energy*, UN, NY, 7,538 (1956)
28. **Grimsrud, E.P. and Kebarle, P.**, Gas phase ion equilibriums studies of the hydrogen ion by methanol, dimethyl ether, and water. Effect of hydrogen bonding. *J. Am. Chem. Soc.* **95**, 7939 (1973)
29. **Dessouki, A.M., El-Assy, N.B., Aly, R.O., Ibrahim, E.H.M. and El-Dossouky, M.M.**, Spectral and gamma-irradiation study of some cyclodiphosphazane compounds. *J. Rad. Nucl. Chem.* **100** (1), 49 (1986)
30. **Becker, G., Colmsjö, A. and Östman, C.**, Elemental composition determination of organophosphorus compounds using gas chromatography and atomic emission spectrometric detection. *Analytical Chimical Acta*, **340**, 181 (1997).
31. **Ying, L.M., Zhi, H.P., Cheng, Z.J., Yi, L. and Xi, X.K.**, Study on syntheses and anti-bacterial activities of some New transition metal Complexes with Schiff base ligand containing pyridine and amide moieties. *Chin. J. Chem.* **22**, 162 (2004).

(Received 27/ 2/ 2011;  
accepted 10/ 11 2011)

## تحضير وتوصيف مركبات فينيل ثيازوليل ايمينو الميثيل وبعض متراكباتها الفلزية المعرضة لأشعة جاما

رؤوف عكاشه على ، رجاء سعد فرج \* ومحمود محمد حسن\*  
المركز القومي للعلوم وتكنولوجيا الاشعاع و\*قسم الكيمياء – كلية العلوم – جامعة الأزهر –  
القاهرة – مصر.

تم تحضير قاعدة "شيف" بتفاعل التكتيف بين الامين 2-امينو-4-فينيل ثيازول والدهيد: ساليسيل الدهيد (I)، اورثو- فثال الدهيدك (II) بنسبة جزيئية 1:1، كما تم تحضير مشتقاتهما الفلزية من  $La^{3+}$ ,  $Zn^{2+}$ ,  $Cu^{2+}$ ,  $Ni^{2+}$ ,  $Co^{2+}$ ,  $Fe^{3+}$ ، كما تم دراسة التركيب الكيميائي لها على اساس من التحليل العنصرى والطيفى للأشعة تحت الحمراء وفوق البنفسجية-المرئية ورنين البروتون المغناطيسى ومطياف الكتلة.

كما تم دراسة فعل التشعيع الجامى باستخدام التحليل الطيفى الفوق بنفسجى- المرئى للمركبات بعد التشعيع وقد تم اقتراح تكون بعض المنتجات اعتماداً على نتائج تحليل مطياف الكتلة، وقد شرحت نتائج التحليل الحرارى الوزنى مستوى الثبات الحرارى للمشتقات الفلزية واكدت كونها.

بالدراسة المشتركة لنتائج التحليل الطيفى بالأشعة فوق البنفسجية – المرئية والخواص المغناطيسية للمشتقات الفلزية أمكن افتراض شيوخ التركيب ثمانى الزوايا للمشتقات عدا المشتق مع فلز النحاس الذى أظهر تشوهاً هندسياً، وقد أعطت معظم المشتقات توصيلية جزيئية منخفضة مما يشير الى دخول الانيونات فى عملية التساهم مع الفلزات وبالتالي السلوك غير الالىكترولىتى .

أظهرت مشتقات النحاس تثبيطاً واضحاً لبكتريا الجرام – الموجية باسيلس سبتيليس (NCTC-1040) إلا أن مشتق النحاس للقاعدة (II) فقط اعطى نفس النتيجة ضد سترىبتوكوكس بيوجينيس (ATCC-19615)، واعطى مشتق الكوبلت للقاعدة (II) نفس النتيجة على بكتريا الجرام- السلبية إى. كولاى وكذلك على الفطر اسبرجيلس فانجاتس.

